Bull Mater Sci (2020)43:301
https://doi.org/10.1007/s12034-020-02233-0

Cation co-doping into ZnS quantum dots: towards visible light sensing applications

G KRISHNAMURTHY GRANDHI[1], MAHESH KRISHNA[2], PAYEL MONDAL[1,3] and RANJANI VISWANATHA[1,2,3,*]

[1]New Chemistry Unit, Jawaharlal Nehru Centre for Advanced Scientific Research, Bangalore 560064, India
[2]International Centre for Materials Science, Jawaharlal Nehru Centre for Advanced Scientific Research, Bangalore 560064, India
[3]School of Advanced Materials, Jawaharlal Nehru Centre for Advanced Scientific Research, Bangalore 560064, India
*Author for correspondence (rv@jncasr.ac.in)

MS received 2 January 2020; accepted 9 April 2020

Abstract. Efficient and environmentally benign visible light responsive materials have been sought after owing to their interesting applications such as visible light photocatalysis, visible light water splitting and visible light sensing. In this research study, the effect of co-doping on the absorption and electrical properties of ZnS quantum dots is studied. Upon co-doping of Fe and Cu into ZnS quantum dots, a new absorption band in the visible region is observed. Furthermore, these quantum dots show photoresponse in the visible region unlike their undoped counterparts that is only effective in the UV region, suggesting their utility in light sensing applications.

Keywords. ZnS quantum dots; co-doping; non-toxic; visible light detection.

1. Introduction

Inorganic semiconducting materials that absorb visible light are of great interest for various applications such as photocatalysis [1,2], solar cells [3,4] and photodetectors [5]. Photodetectors with UV–visible–NIR spectral response have gained great attention due to their various applications in image sensing, communication and environmental monitoring [6,7]. Crystalline Si is one of the most studied systems that has been used for visible light detection [8]. However, its limitations like its weak absorption over the entire spectrum have limited its use in photodetectors. Oxide semiconductors have been found to be good candidates to replace Si in many electrical devices [9]. However, oxide semiconductor-based devices are transparent due to their very high band gap and hence limited to UV light detection [10]. Efforts have been made to improve the visible light response of these oxide semiconductors to some extent with the help of a polymer material as the light-absorbing layer [11]. They were also used by blending with semiconductor quantum dots (QDs) [12]. For example, p-type doping in NiO results in visible light sensing [5]. Other than these oxide materials, there are extensive reports on the UV-based photodetectors which are based on high band gap materials such as TiO_2, ZnO and ZnS nanostructures [13–15]. Semiconductor materials like CdS [16], ZnTe [17] and In_2S_3 [18] show visible photoresponse while InGaAs [19], InAs [20] and Cd_3P_2 [21] are good for NIR light detection. However, most of these visible and NIR photodetector materials are toxic in nature. Hence, there still exists a demand for the development of visible light-sensitive materials made up of earth abundant and low toxic elements.

Among all the approaches made to date, one of the approaches to attain visible light-sensitive materials is by altering the properties of UV-absorbing materials like ZnO, TiO_2 and ZnS such that they show visible photoresponse. It was shown in the literature that heavy doping into UV-absorbing materials, such as ZnO and TiO_2 strongly affects their band gap [22–24]. For example, varying the concentration of Al doping results in tunable band gap in ZnO nanocrystalline thin films. This leads to tunable wavelength photoresponse with increasing Al dopant concentration [24]. Other important options include anion doping that introduces dopant subbands on top of VB [23,25] or the cation doping to affect the CB position [26], which leads to reduction of the band gap. From this perspective, the anion mono-doping or even co-doping into semiconductor materials to alter the electronic structure of host material is studied more extensively than that of cation doping. Cation co-doping, particularly in QDs, is not much studied to the best of our knowledge. In this research study, we tuned the optical properties of high band gap

This article is part of the Topical Collection: SAMat Focus Issue.
Published online: 20 November 2020

material ZnS QDs by co-doping with Cu and Fe synthesized using wet-colloidal method and show their improved visible light sensing.

2. Experimental

2.1 *Materials*

CuI, iron acetylacetonate, zinc acetate, zinc stearate, S powder, dodecanethiol (DDT), oleic acid (90%), oleylamine (70%), trioctylphosphine (TOP, 90%) and 1-octadecene (ODE, 90%) were purchased from Sigma-Aldrich. Hexane, methanol and acetone were obtained from SD Fine chemicals. All the purchased chemicals were used without any further purification.

0.2 M zinc oleate was prepared by heating 0.37 g of zinc acetate to 200°C in the presence of 1.13 g of oleic acid and 7 ml of ODE to form a clear solution. Once zinc oleate is formed, the reaction mixture was cooled down to room temperature. Approximately, 3 ml of oleylamine is added to the reaction mixture to prevent the solidification of zinc oleate solution at room temperature. ZnS precursor solution was obtained by mixing 6 ml of zinc oleate with 2.5 ml of DDT and 2 ml of oleic acid at room temperature.

2.2 *Synthesis of Cu-doped, Fe-doped and co-doped ZnS QDs*

CuI (0.1 mmol, 19 mg), iron acetylacetonate (0.1 mmol, 35 mg) and oleylamine (10 ml) were degassed in a three-necked flask for 1 h at 80°C and then the reaction mixture was back-filled with Ar. The temperature of the reaction was raised to 250°C followed by the swift injection of 2 ml of TOP into the reaction mixture. Then, the reaction mixture was annealed for 2 h at this temperature. After 2 h, ZnS precursor solution was added to the reaction mixture in a drop-wise manner, thrice at regular intervals of 45 min. After addition of complete ZnS solution into the reaction mixture, the reaction mixture was annealed for 4–5 h until it turned into a thick black-coloured solution. The sample was washed using hexane/methanol mixture and then precipitated by adding excess of acetone. The Cu- and Fe-doped ZnS QDs were synthesized using the procedure similar to the co-doped QDs. The undoped ZnS QDs were prepared by heating zinc stearate and S in ODE at 270°C.

2.3 *Characterization and spectroscopic techniques*

Crystal structure identification of the particles was carried out using X-ray diffraction (XRD), recorded on Bruker D8 Advance diffractometer using Cu K_α radiation. Since the diffracted intensities from these QDs are generally weak, all patterns were recorded at a slow scan rate (0.75° per minute) in order to obtain a high signal-to-noise ratio. The bulk XRD pattern was obtained from the inorganic crystal structure database (ICSD). Crystal structure and size identification of the QDs were carried out using XRD and transmission electron microscopy (TEM). TEM images were recorded using a Technai F30UHR version electron microscope, using a field emission gun (FEG) at an accelerating voltage of 300 kV. Samples for TEM were prepared by adding a solution of the QDs dissolved in hexane dropwise on a carbon-coated Cu grid. The solution was allowed to evaporate, leaving behind the QDs. UV–visible absorption spectra of various aliquots dissolved in hexane, chloroform and methanol were obtained using an Agilent 8453 UV–visible spectrometer. Inductively coupled plasma optical emission spectroscopy (ICP-OES) was used to determine Cu to Zn and Fe to Zn ratios in the doped and co-doped ZnS QDs. QDs were washed to remove excess precursors and then digested in concentrated HNO_3 and diluted with Millipore water. ICP-OES was carried out using a Perkin Elmer Optima 7000 DV machine.

2.4 *Dark and photoresponse measurements of undoped and co-doped QDs*

I–V characteristics of undoped ZnS as well as Cu and Fe co-doped ZnS QDs were measured with a solar simulator (Newport, model: 91160-1000, 300 W Xe lamp) equipped with AM 1.5 G filter with the simulated light intensity adjusted to 100 mW cm^{-2}. The sample is coated on a fluorine-doped tin oxide (FTO) substrate and the Au electrodes were used as contacts from the sample to the source meter.

2.5 *Device fabrication*

The FTO-coated glass substrates were procured from Sigma Aldrich and cut into (1.5 × 1.5) cm^2 size to be used as the transparent conducting electrode. The FTO plates were cleaned using ultrasonication by a four-step procedure namely; sonication in 10% aqueous sodium dodecyl sulphonate (SDS) for 10 min followed by deionized water for 10 min. It was then sonicated in anhydrous ethanol for 10 min and finally in hexane for 10 min. The FTO-coated glass slides were dried under a gentle flow of warm dry air (50°C). UV–visible absorption spectra of the blank substrates were measured to ensure the glass plates were spectroscopically clean. The FTO plates were patterned by etching using zinc dust and 1 M HCl mixture with the help of appropriate masks to separate the electrodes and active phase and prevent short circuit.

The photodetector was fabricated using a custom-built spin coater. The spin coater consists of three parts: a DC motor, a voltage regulator and a sample mount. The DC motor was rated at 12 V, 1.5 A with a rated speed of 3000 rpm. The motor was mounted on a vibration damping

platform constructed using soft materials such as Styrofoam. Hamilton 100 µl syringe was used to manually spin cast the QDs. Voltage regulator was used to vary the speed. Briefly, the configuration chosen for our device was glass/FTO/QDs/Au with the glass side used for illumination. 10 ml of the respective QD solution dispersed in hexane was spin coated on to the FTO-coated glass in a home-built spin coater set to a rotation speed of 2500 rpm using 30 µl per cycle of film growth. One cycle of growth consists of rapid injection at 500 rpm and spinning at 2500 rpm for 30 s to allow the QDs to dry and the film to grow. Thereafter, 400 nm thick gold electrodes were physical vapour-deposited onto the QDs-coated slides. The *I–V* characteristics were measured using a Keithley 2600 type source meter. Aperture of 4×4 mm^2 prepared from aluminium foil was used to restrict the illuminated area to the centre of the film.

3. Results and discussion

Cu and Fe co-doped QDs were synthesized by adding ZnS precursor to the solution containing Cu and Fe in the presence of oleylamine as explained in the experimental section. The formation of the QDs was confirmed by XRD studies as shown in figure 1a. The XRD pattern of the QDs synthesized matches well with the cubic phase of ZnS, as

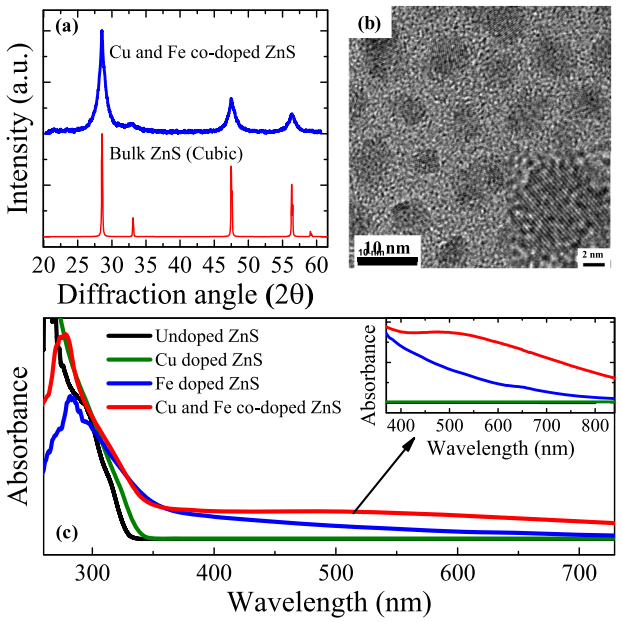

Figure 1. Structural and optical properties of the QDs. (**a**) XRD pattern of Cu and Fe co-doped ZnS QDs along with the bulk cubic ZnS pattern from the ICSD database. (**b**) TEM image of Cu and Fe co-doped ZnS QDs. Inset shows the high-resolution TEM image of the co-doped QDs. (**c**) Absorption spectra of the undoped, Cu-doped, Fe-doped and co-doped ZnS QDs and the inset show the magnified portion of the spectra of the QDs in the visible region.

obtained from the ICSD database. The presence of broad peaks in the XRD pattern of doped dots compared to the bulk XRD pattern as shown in figure 1a suggests the formation of smaller particles. The formation of small particles was further confirmed from TEM image as shown in figure 1b. The average size of the particles is estimated to be around 5–6 nm and the size distribution of the particles is small as observed from the figure. The high crystallinity of these particles is also observed from the high-resolution TEM analysis (inset of figure 1b). Elemental analysis (ICP-OES) was performed on these NCs and doping of both Cu (6%) and Fe (5%) into ZnS lattice was confirmed. The effect of doping on the optical properties of the QDs was studied. Figure 1c shows the absorption spectra of the undoped and doped ZnS QDs. The undoped ZnS QDs (black curve in the figure) exhibit an absorption band in the UV regime (absorption maximum is at $\sim$315 nm). This UV absorption band would be attributed to the electronic transition between conduction band (CB) and valence band (VB) of ZnS QDs [27,28]. On the other hand, the co-doped sample (red line) shows an additional band in the visible regime around 500 nm along with the absorption band observed for the undoped counterpart. The presence of the visible absorption band is highlighted in the inset of figure 1c. However, the visible absorption band might arise owing to the co-doping or due to either Cu-only or Fe-only doping. Therefore, we have also compared the absorption spectrum of co-doped QDs with that of Fe-doped and Cu-doped QDs (figure 1c). Cu-doped QDs only absorb in the UV regime similar to the undoped QDs, indicating that, Cu doping alone cannot affect the band gap or electronic structure of ZnS QDs. Fe doping in ZnS QDs results in appearance of featureless and feeble absorption tail in the visible regime of the absorption spectrum as shown in the inset of figure 1c. However, this absorption feature is not as strong as in case of co-doped QDs indicating that the absorption feature around 500 nm present in the co-doped sample appeared only as a result of co-doping. Furthermore, either the appearance of additional visible absorption bands or shift in the host band gap towards visible wavelengths were reported for Cu^{2+}/Ga^{3+}, Ag^{+}/In^{3+} and Mn^{2+}/Sm^{3+} co-doped ZnS QDs previously [29–31]. Additionally, it has been well established from density functional theory that upon doping with transition metal elements, it gives rise to mid-gap states. Specifically with Fe, it gives a large number of mid-gap states which increases with other dopants [32]. Therefore, the additional broad absorption band around 500 nm observed in the co-doped ZnS QDs in this study would be attributed to the charge transfer between CB or VB of host and the dopant levels in the host band gap or the vacancy levels formed by the doping of both Cu^{2+} and Fe^{3+} ions. Furthermore, a downwards shift in the CB position of the host is possible upon heavy co-doping ($\sim$10%) [26]. The co-doped ZnS QDs also contain the UV absorption band similar to the undoped QDs and this might be due to the inherent nature of the co-doped dots with two absorption

bands or the UV absorption band might have arisen from the undoped portion present in the co-doped sample.

Furthermore, we have not observed any emission properties for the co-doped ZnS QDs. This might be because of the following reasons. The transition metal ion (such as Cu^{2+} and Mn^{2+}) doping can result in appearance of dopant-related emission in II-VI semiconductor QDs [33]. However, the dopant emission efficiency depends upon various parameters such as doping percentage, environment around dopant ions in the host and the distribution of dopants. Additionally, Fe^{3+} dopants are known to completely quench the photoluminescence intensity of II-VI QDs [34].

As the co-doped QDs have a broad absorption in the visible regime, we have studied the *I–V* characteristics of the undoped, and co-doped samples as shown in figure 2. The device structure is shown in the inset of this figure. The device is illuminated from the FTO side and the experiment is explained in the experimental section. Figure 2a–c show the *I–V* characteristics of undoped, Fe-doped and co-doped ZnS QDs, respectively, in the dark and with the illumination of light. It can be observed that all of them displayed enhancement of current when they are illuminated with the Xe lamp compared to the dark response. Nevertheless, the enhancement of current in the presence of light (photocurrent) is nearly 3 times higher in case of co-doped QDs when compared to both undoped and Fe-doped ZnS QDs, as shown in figure 2. Also, since Cu is an optically active dopant, with specific states [35] rather than a large number of acceptor states like in Fe, we do not observe any change in the photoresponse. The higher photoresponse of the co-doped QDs might be a consequence of their ability to absorb both UV and visible light compared to undoped and single-dopant ZnS QDs, which absorb only in the UV regime. This is consistent with the other visible light absorbing co-doped ZnS QDs, which were utilized for visible-light-induced applications such as hydrogen production [29,30].

However, there exists an extra visible absorption band in the co-doped QDs, which is not present in the undoped

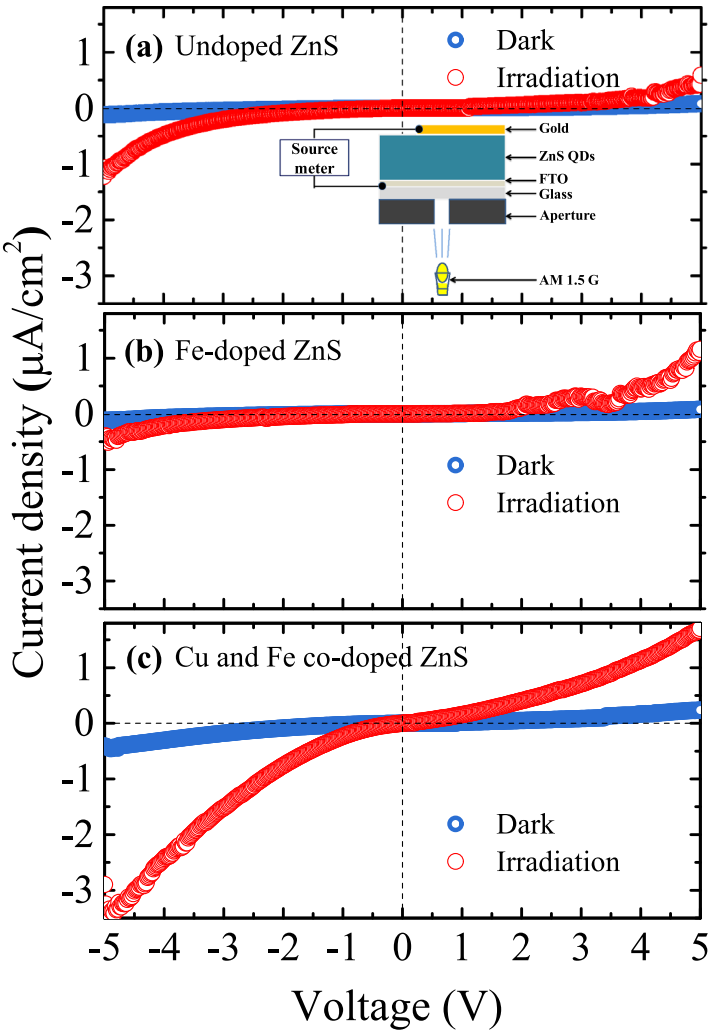

Figure 2. The *I–V* characteristics of (**a**) undoped, (**b**) Fe-doped and (**c**) co-doped QDs in the dark and with the irradiation of light using Xe lamp. The inset of (**a**) shows the device structure.

QDs. To realize the contribution of this visible absorption band to the photoresponse of these co-doped QDs (shown in figure 2c), their photoresponse was measured by using cut-off filters of varying wavelengths which block the light of shorter wavelengths than the wavelength labelled on the filter as shown in figure 3. For example, a 450-nm filter only allows the photons of wavelengths greater than 450 nm.

In case of undoped QDs, the photocurrent gradually decreases with increasing the wavelength of cut-off filters as shown in figure 3a. There is a decrease in photoresponse even with a 450-nm filter and it decreases drastically with further increase in the wavelength of the cut-off filters. This suggests that undoped ZnS QDs are effective only in UV regime. On the other hand, as the Fe-doped QDs also show a weak absorption feature in the visible regime (inset of figure 1c), their photocurrents with increase in the wavelength of cut-off filters are measured as shown in figure 3b. It is found that the photoresponse starts diminishing even with 495 nm filter and thereafter it further decreases with increase in the wavelength of the filter. This suggests that Fe-doped ZnS QDs do not show any appreciable light response in the visible regime. Finally, the photoresponse of the co-doped QDs in the visible region is shown in figure 3c. The photoresponse is almost unchanged even with the use of 590-nm filter but thereafter it diminishes. So, the co-doped QDs exhibit improved visible light response unlike the undoped counter parts which are only UV light sensitive. This shows that Cu and Fe co-doped ZnS QDs can be good candidates for visible light detection than the undoped or Cu- or Fe-doped ZnS QDs.

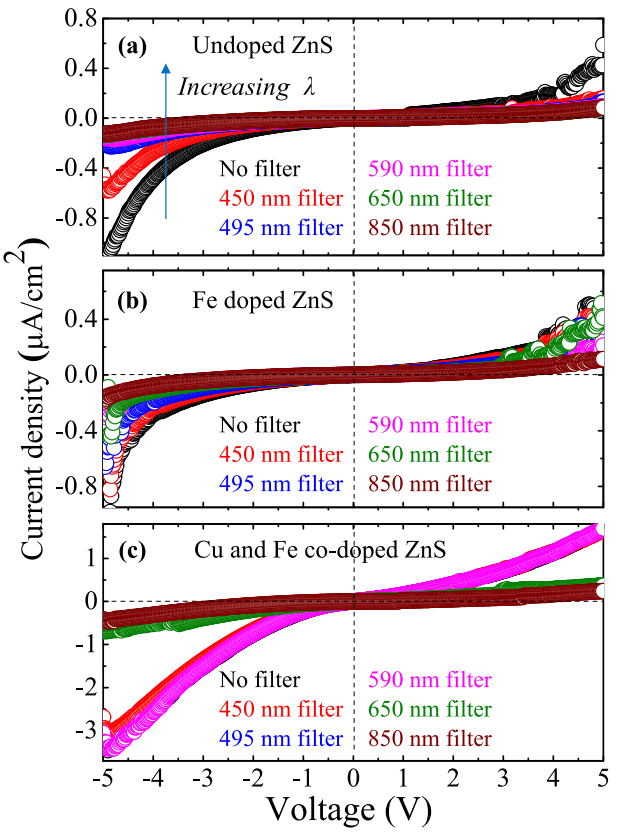

Figure 3. The photoresponse of (**a**) undoped, (**b**) Fe doped and (**c**) co-doped ZnS QDs by using light cut-off filters of different wavelengths.

4. Conclusions

Cu and Fe co-doped ZnS QDs were synthesized using hot injection method. The co-doping results in the appearance of a new visible absorption band for ZnS QDs. The co-doped QDs show visible photoresponse whereas their undoped or singly doped counterparts are only effective in the UV region. These QDs might be viable candidates for non-toxic and environmentally benign visible photodetectors.

Acknowledgements

We acknowledge JNCASR, Sheikh Saqr Laboratory and Department of Science and Technology, Government of India for financial support. GKG and PM thank CSIR for a research fellowship.

References

[1] Zong X, Yan H, Wu G, Ma G, Wen F, Wang L *et al* 2008 *J. Am. Chem. Soc.* **130** 7176
[2] Asahi R, Morikawa T, Ohwaki T, Aoki K and Taga Y 2001 *Science* **293** 269
[3] Kojima A, Teshima K, Shirai Y and Miyasaka T 2009 *J. Am. Chem. Soc.* **131** 6050
[4] Santra P K and Kamat P V 2012 *J. Am. Chem. Soc.* **134** 2508
[5] Mallows J, Planells M, Thakare V, Bhosale R, Ogale S and Robertson N 2015 *ACS Appl. Mater. Interfaces* **7** 27597
[6] Konstantatos G and Sargent E H 2010 *Nat. Nanotech.* **5** 391
[7] Konstantatos G, Clifford J, Levina L and Sargent E H 2007 *Nat. Photon.* **1** 531
[8] Mridha S and Basak D 2007 *J. Appl. Phys.* **101** 083102
[9] Sakai T, Seo H, Aihara S, Kubota M, Egami N, Wang D *et al* 2012 *Jpn. J. Appl. Phys.* **51** 010202
[10] Chang T H, Chiu C J, Chang S J, Tsai T Y, Yang T H, Huang Z D *et al* 2013 *Appl. Phys. Lett.* **102** 221104
[11] Zan H-W, Chen W-T, Hsueh H-W, Kao S-C, Ku M-C, Tsai C-C *et al* 2010 *Appl. Phys. Lett.* **97** 221104
[12] Liu X, Yang X, Liu M, Tao Z, Dai Q, Wei L *et al* 2014 *Appl. Phys. Lett.* **104** 113501
[13] Wang X, Xie Z, Huang H, Liu Z, Chen D and Shen G 2012 *J. Mater. Chem.* **22** 6845
[14] Hu L, Yan J, Liao M, Xiang H, Gong X, Zhang L *et al* 2012 *Adv. Mater.* **24** 2305
[15] Game O, Singh U, Kumari T, Banpurkar A and Ogale S 2014 *Nanoscale* **6** 503
[16] Li H, Wang X, Xu J, Zhang Q, Bando Y, Golberg D *et al* 2013 *Adv. Mater.* **25** 3017

[17] Liu Z, Chen G, Liang B, Yu G, Huang H, Chen D *et al* 2013 *Opt. Express* **21** 7799
[18] Xie X and Shen G 2015 *Nanoscale* **7** 5046
[19] Tan H, Fan C, Ma L, Zhang X, Fan P, Yang Y *et al* 2016 *Nano-Micro Lett.* **8** 29
[20] Miao J, Hu W, Guo N, Lu Z, Zou X, Liao L *et al* 2014 *ACS Nano* **8** 3628
[21] Yang C, Pan H, Liu S, Miao S, Zhang W-H, Jie J *et al* 2015 *Chem. Commun.* **51** 2593
[22] Qin H, Li W, Xia Y and He T 2011 *ACS Appl. Mater. Interfaces* **3** 3152
[23] Kouser S, Lingampalli S R, Chithaiah P, Roy A, Saha S, Waghmare U V *et al* 2015 *Angew. Chem. Int. Ed.* **54** 8149
[24] Chongsri K and Pecharapa W 2014 *Energy Proc.* **56** 554
[25] Gai Y, Li J, Li S-S, Xia J-B and Wei S-H 2009 *Phys. Rev. Lett.* **102** 036402
[26] Long R and English N J 2011 *Appl. Phys. Lett.* **98** 142103
[27] Saravanan R S S, Pukazhselvan D and Mahadevan C 2012 *J. Alloys Compd.* **517** 139
[28] Li L S, Pradhan N, Wang Y and Peng X 2004 *Nano Lett.* **4** 2261
[29] Kimi M, Yuliati L and Shamsuddin M 2015 *J. Nanomater.* **2015** 1
[30] Kimi M, Yuliati L and Shamsuddin M 2014 *Adv. Mater. Res.* **1024** 368
[31] Prasanth S, Irshad P, Raj D R, Vineeshkumar T, Philip R and Sudarsanakumar C 2015 *J. Lumin.* **166** 167
[32] Akhtar M S, Riaz S and Naseem S 2015 *Mater. Today: Proc.* **2** 5528
[33] Srivastava B B, Jana S, Karan N S, Paria S, Jana N R, Sarma D *et al* 2010 *J. Phys. Chem. Lett.* **1** 1454
[34] Saha A, Makkar M, Shetty A, Gahlot K, Pavan A and Viswanatha R 2017 *Nanoscale* **9** 2806
[35] Grandhi G K, Tomar R and Viswanatha R 2012 *ACS Nano* **6** 9751